

B.L. Miller, D.G. Vincent and D.M. Kann
Department of Geosciences
Purdue University
West Lafayette, IN 47907

Franklin R. Robertson
Systems Dynamics Lab
NASA/MSFC/ED42
Huntsville, AL 35802

1. INTRODUCTION

Cyclone development and movement in the South Pacific have long been recognized. Data regarding cyclone activity originally stemmed from island and merchant ship reports and was enhanced by research programs, such as the IGY. With the advent of the meteorological satellite in the 1960's, knowledge concerning South Pacific cyclones was further enhanced. Of particular interest in the present study, are the cyclones which form and propagate in and along the South Pacific Convergence Zone (SPCZ). The climatology of these cyclones has been documented by several authors (e.g., Troup and Streten, 1972; Streten and Troup, 1973). A general account of cyclone activity within the SPCZ, which is most appropriate for the present study, is given by Trenberth (1976). A more detailed description of the particular cyclone events which are alluded to herein is given by Vincent (1985).

The focus of the present paper is twofold. First, it examines the heat budget of the tropical South Pacific for the period, 10-18 January 1979, and compares precipitation estimates obtained from the budget equation to those derived from GOES IR satellite imagery. Second, it looks at the relationship between latent heat release and the baroclinic energy conversion during the life cycles of two cyclones which propagate along the SPCZ in the period. The data sources used in this study are part of the total FGGE data package and include: a modified set of Level III-b upper air analyses originally produced at ECMWF; surface observations from island stations, mobile ships and drifting buoys in the South Pacific; GOES-West enhanced IR satellite imagery; and outgoing longwave radiation (OLR) estimates deduced from NOAA polar-orbiting satellites. Further descriptions of these data, as they apply to the present study, appear in Vincent (1982, 1985). It should be noted that without the FGGE data set the details regarding the circulation features associated with the present study would have been greatly reduced.

One of the main equations used in this investigation is the atmospheric heat budget equation:

$$Q_1 = \frac{\partial s}{\partial t} + \vec{V} \cdot \nabla s + \omega \frac{\partial s}{\partial p} \quad (1)$$

where $s = c_p T + gz$, the dry static energy and Q_1 is the apparent heat source (Yanai et al., 1973), composed of the net radiation (QR), sensible heat exchange with the earth's surface (QS), and latent heat release (QL). In (1), terms on the right side were calculated from the aforementioned ECMWF analyses at mandatory pressure levels from 1000-100 mb and at horizontal increments of 2.5° lat/lon using 0000 and 1200 GMT data. On the left of (1), a vertical profile for QR was selected based on the results obtained by Cox and Griffith (1979) for the GATE area during Phase III. The spatial and temporal conditions for their study are similar to those for the present case. Values of QS in (1) were computed using the Bulk Aerodynamic Method (Bunker, 1976) and applied to the 1000-850 mb layer. Sea surface temperatures for that method were obtained from weekly averages based on polar orbiting satellite measurements for the period 9-16 January. The final term in (1), QL, was deduced as the residual. Thus, it represents the latent heat release, and inherits any errors and subgrid-scale contributions from terms in (1).

2. RESULTS AND DISCUSSION

From 10-18 January the SPCZ was quasi-stationary and convectively active (Vincent, 1982). The mean position of the cloud band ($OLR \leq 225 \text{ Wm}^{-2}$) associated with the SPCZ for this period is shown in Fig. 1, together with the mean position of surface pressure. Note that the trough of low pressure is located along the southern and western edge of the SPCZ. This trough marks the axis along which the SPCZ cyclones propagate in a southeastward direction, having their warm sector within the cloud band and their cold sector to its southwest. Also shown in Fig. 1 is the chart of mean sea level pressure for 0000 GMT 12 January which depicts three cyclones. Vincent (1985) gives a detailed discussion of the characteristics and kinematics of each cyclone during its life cycle. At this time, L_2 is propagating southeastward and is in its late formative stage; twelve hours later it was a mature cyclone. L_3 is quasi-stationary and is in its early wave stage, having just attained a closed surface circulation. About two days later, L_3 propagates into middle latitudes along the same path as for L_2 . The third cyclone, L_1 , remained in the tropics throughout its life cycle (10-14 January) and propagated slowly eastward. The rainfall patterns shown in

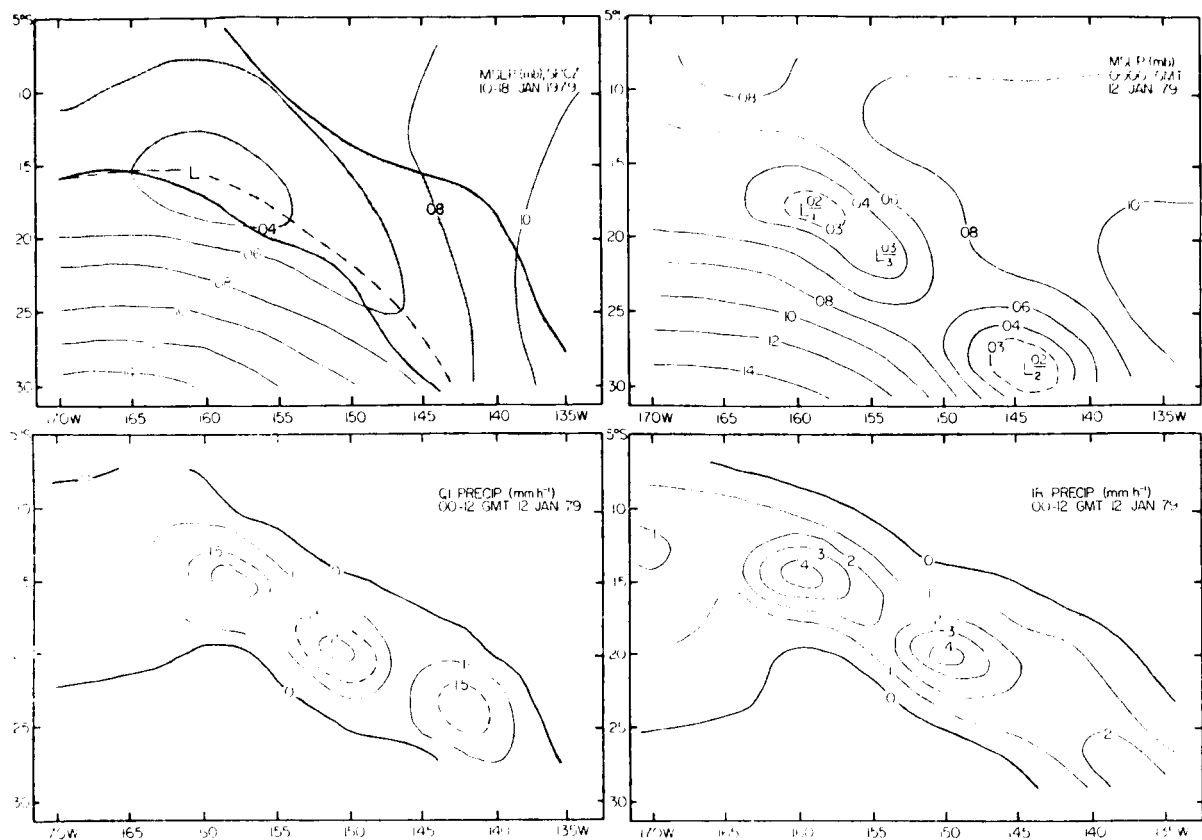


Fig. 1. Time-averaged mean sea level pressure for 10-18 January 1979 with outgoing longwave radiation values of $\leq 225 \text{ Wm}^{-2}$ shaded to represent the SPCZ (upper left); mean sea level pressure for 0000 GMT 12 January 1979 with location of three surface cyclones (upper right); precipitation rates derived from Q1 budget (lower left) and IR satellite method (lower right) for 12 h period, 0000-1200 GMT 12 January 1979.

Fig. 1 suggest that the heaviest precipitation occurs in conjunction with the cyclones. Two estimates of precipitation rates are depicted in Fig. 1 for the 12 h period, 0000-1200 GMT 12 January: (1) those obtained as the residual in the heat budget (Eq. 1) and (2) those derived from enhanced IR satellite cloud top temperatures (Robertson, 1985). It is seen that the patterns are in reasonable agreement, but that the magnitudes are about 2 times larger by the satellite method. It should be noted that values obtained by both methods were for 2.5° lat/lon areas. The satellite estimates were derived from data which originally was at 3 h increments and 16 km image resolution.

A comparison of the area-averaged 12 hourly precipitation rates between the heat budget and satellite methods is given in Fig. 2. Three sets of time-series curves are shown. One set depicts the area-averaged rainfall for the total area over which the heat budget results were calculated, $7.5\text{--}27.5\text{S}$, $170\text{--}135\text{W}$. In this set, zero values have been included. A second set shows the percentage of the total area occupied by precipitating clouds, while the third set gives the average rainfall rates for precipitating areas only. The time means of the total area results for the 9-day period are in good

agreement between the two methods, although, in general, the satellite values are greater early in the period, while the heat budget values are greater after 1200 GMT 13 January. As inferred from Fig. 1, the satellite value in Fig. 2 on 12 January is about twice that derived from the heat budget. It's worth noting that even though the magnitudes between the two methods differ by a greater amount in the early part of the period, the patterns are typically in good agreement. Toward the end of the period, the patterns are not in as good agreement, but the area-averaged results are more comparable. Figure 2 shows that the percentage of the total area containing precipitating clouds is generally greater by the heat budget method, particularly after the first few days. This is not too surprising since the heat budget relies on large-scale data and, to a great extent, on moisture convergence; thus, the method would tend to overestimate the area of precipitation. On the other hand, the satellite method yields precipitation values only where relatively cold cloud top temperatures exist and it utilizes a considerably smaller horizontal scale of resolution in the initial data compilation (Robertson, 1985). For these same reasons, it's also not surprising that the average values of rainfall rates within the precipitating clouds are

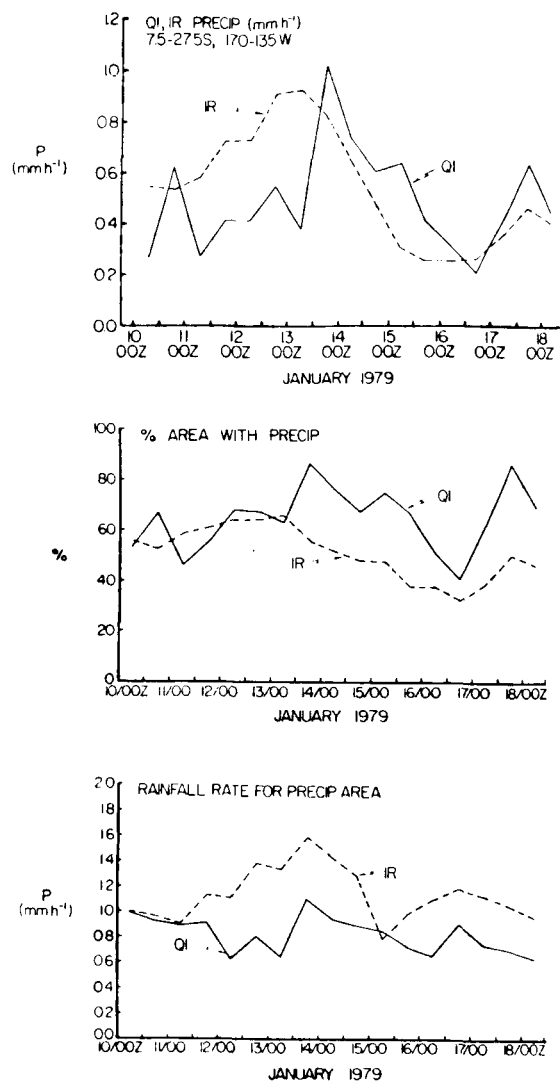


Fig. 2. Time series of area-averaged precipitation rates by QI and IR satellite methods (upper panel), percentage of area occupied by precipitating grid points (middle panel), and rainfall rates for precipitating area only (lower panel).

greater when derived by the satellite method (Fig. 2).

The significance of each of the terms in (1) is shown in Fig. 3 which illustrates their time-averaged vertical distribution for the total area. The terms that make the most significant contributions to the heat budget are net radiation, which acts as a sink, and the vertical advection of dry static energy which is a source. Since radiative cooling is nearly constant with height from 850–200 mb, the shape of the residual curve, which represents latent heat, is similar to that for vertical advection. Maximum latent heat release occurs in the 500–400 mb layer with a value slightly in excess of $6 \times 10^{-2} \text{ W kg}^{-1}$ (5 K d^{-1}). The relative significance of terms and the vertical distribution of latent heat at individual times were similar to

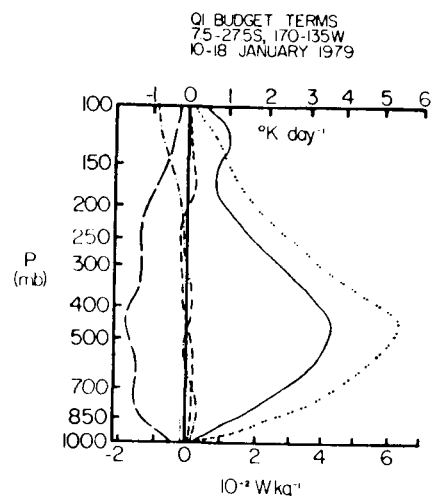


Fig. 3. Vertical distribution of time-averaged and area-averaged terms in the QI budget for 10–18 January 1979. Terms depicted are: net radiation, QR (long dash), local rate of change (short dash), horizontal advection (dash-dot), vertical advection (solid), and latent heat release, QL (double dot).

those for the composite. Furthermore, preliminary results of the vertical distribution of latent heating, currently being derived for the satellite method by Robertson (personal communication), indicate a good agreement with the heat budget results.

As anticipated, latent heat serves an important role within a cyclone system. It's well known that latent heat generally serves as the primary diabatic component for generating potential energy. It can also play an important role in the baroclinic energy conversion between potential and kinetic energy through diabatically-induced vertical circulations, i.e., relatively warm air rising and/or cold air sinking. Figure 4 shows a time series of the 12-hourly area-averaged values of the baroclinic conversion, $\overline{\omega T}$, for two of the three cyclones mentioned earlier (Fig. 1). The particular cyclone systems of interest are the ones which propagated into mid-latitudes, L₂ and L₃. A perusal of some of the horizontal distributions of observed and computed variables (e.g., surface pressure, divergence, relative vorticity, cloud top temperatures, OLR), suggested that each cyclone system could be represented by a box which was 20° latitude by 20° longitude. Thus, the results shown in Fig. 4 have been area-averaged over a moving frame of reference, 20° lat/lon, centered on the surface position of the low pressure center. It is seen that the conversion increases with time for L₂, whereas it decreases with time for L₃. Vincent (1985) found that the former cyclone system intensified, while the latter one weakened. Figure 4 shows that the percentage of the first system's area occupied by precipitating clouds (according to the satellite estimates) remained nearly constant at about 60% throughout the cyclone's life cycle. In contrast, the precipitation area

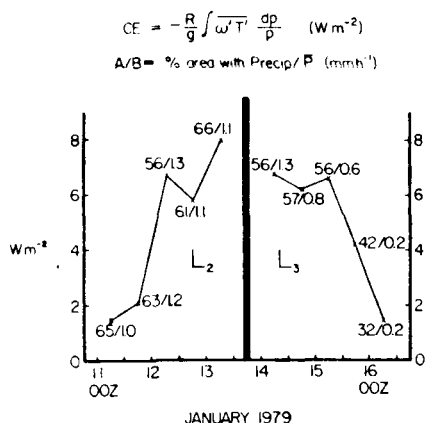


Fig. 4. Baroclinic energy conversion, CE, for cyclone vicinity (20° lat/lon centered on surface cyclone) for L_2 and L_3 . Also shown are percentage of cyclone area occupied by precipitating grid points and the average rainfall rate for the precipitating area.

for the second cyclone decreased from 56% during its mature stage to 32% in its dissipation stage. Perhaps more important is the difference between the mean values of the rainfall rate achieved by precipitating clouds within each cyclone system. For L_2 it remained relatively steady at about 1.2 mm h^{-1} , but for L_3 it decreased steadily from 1.3 mm h^{-1} during the cyclone's formation stage, to 0.6 mm h^{-1} by its mature stage, and finally to 0.2 mm h^{-1} in its late mature and dissipating stage. Thus, for the cyclone where latent heat stays at a high level, both spatially and with regard to intensity, there appears to be ample fuel for its intensification. On the other hand, for the filling cyclone, the latent heat impact decreases and the baroclinic conversion falls off rapidly, presumably due to the lack of both potential energy generation and diabatically-induced thermally-direct circulations. Work currently is in progress to determine the importance of latent heat on the vertical motion field and, thus, on the baroclinic energy conversion.

ACKNOWLEDGEMENTS

The authors thank Drs. Julia Paegle and John Ward for their assistance in supplying them with the ECMWF data and Dr. Huo-Jin Huang for his help, both in scientific discussions and computer programming. Also, they appreciate the help provided by Mr. Douglas Miller who drafted the figures and Ms. Helen Henry who typed the manuscript. The research was sponsored by the Global Atmospheric Research Program, Division of Atmospheric Science, National Science Foundation and the National Oceanic and Atmospheric Administration under Grant Number ATM 8505748 and by the National Aeronautics and Space Administration under Contract Number NAS8-35187.

REFERENCES

- Bunker, A.F., 1976: Computations of surface energy flux and air-sea interaction cycles of the North Atlantic Ocean. *Mon. Wea. Rev.*, 104, 1122-1140.
- Cox, S.K. and K.T. Griffith, 1979: Estimates of radiative divergence during Phase III of GARP Atlantic Tropical Experiment: Part II. Analyses of Phase III results. *J. Atmos. Sci.*, 36, 586-601.
- Robertson, F.R., 1985: IR precipitation estimates in the South Pacific during FGGE SOP-1. Preprint, Sixteenth Conference on Hurricanes and Tropical Meteorology, May 14-17, 1985, Houston, TX, American Meteorological Society, Boston, MA, 02108, 2 pp.
- Streten, N.A. and A.J. Troup, 1973: A synoptic climatology of satellite-observed cloud vortices over the southern hemisphere. *Quart. J. Roy. Meteor. Soc.*, 99, 56-72.
- Trenberth, K.E., 1976: Spatial and temporal variations of the Southern Oscillation. *Quart. J. Roy. Meteor. Soc.*, 102, 639-653.
- Troup, A.J. and N.A. Streten, 1972: Satellite-observed Southern Hemisphere cloud vortices in relation to conventional observations. *J. Appl. Met.*, 11, 909-917.
- Vincent, D.G., 1982: Circulation features over the South Pacific during 10-18 January 1979. *Mon. Wea. Rev.*, 110, 981-993.
- , 1985: Cyclone development in the South Pacific Convergence Zone during FGGE, January 1979. *Quart. J. Roy. Meteor. Soc.*, 111, 155-172.
- Yanai, M., S. Esbensen and J.H. Chu, 1973: Determination of bulk properties of tropical cloud clusters from large-scale heat and moisture budgets. *J. Atmos. Sci.*, 30, 611-627.